



# Long term effects of cueing procedural memory reactivation during NREM sleep

Martyna Rakowska\*, Mahmoud E.A. Abdellahi, Paulina Bagrowska<sup>1</sup>, Miguel Navarrete<sup>2</sup>, Penelope A. Lewis

Cardiff University Brain Research Imaging Centre (CUBRIC), School of Psychology, Cardiff University, Maindy Rd, Cardiff CF24 4HQ, UK



## ARTICLE INFO

### Keywords:

Sleep  
Targeted memory reactivation  
Long-term memory  
Procedural memory  
SO-Spindle coupling  
consolidation

## ABSTRACT

Targeted memory reactivation (TMR) has recently emerged as a promising tool to manipulate and study the sleeping brain. Although the technique is developing rapidly, only a few studies have examined how the effects of TMR develop over time. Here, we use a bimanual serial reaction time task (SRTT) to investigate whether the difference between the cued and un-cued sequence of button presses persists long-term. We further explore the relationship between the TMR benefit and sleep spindles, as well as their coupling with slow oscillations. Our behavioural analysis shows better performance for the dominant hand. Importantly, there was a strong effect of TMR, with improved performance on the cued sequence after sleep. Closer examination revealed a significant benefit of TMR at 10 days post-encoding, but not 24 h or 6 weeks post-encoding. Time spent in stage 2, but not stage 3, of NREM sleep predicted cueing benefit. We also found a significant increase in spindle density and SO-spindle coupling during the cue period, when compared to the no-cue period. Together, our results demonstrate that TMR effects evolve over several weeks post-cueing, as well as emphasising the importance of stage 2, spindles and the SO-spindle coupling in procedural memory consolidation.

## 1. Introduction

The essential role of sleep in memory processing is supported by a multitude of studies (for reviews see [Diekelmann and Born 2010](#), [Rasch and Born 2013](#) and [Dudai 2012](#)). Both declarative (summarised in [Gais and Born 2004](#)) and procedural (summarised in [Loganathan 2014](#)) memory consolidation benefit from sleep. Memory reactivation, wherein a pattern of brain activity elicited during learning re-emerges during subsequent sleep, is thought to be the mechanism underpinning this process ([Born et al., 2006](#)). Although first discovered in rodents ([Wilson and McNaughton, 1994](#)), the phenomenon was also evidenced to occur in humans, where its magnitude predicts the next-day memory improvements ([Peigneux et al., 2004](#)). Recently, a procedure known as targeted memory reactivation (TMR) emerged as a promising tool to manipulate and study the mechanisms of memory reactivation. In a typical TMR experiment, a tone or an odour previously associated with a newly encoded memory is covertly re-presented during sleep (e.g., [Rasch et al. 2007](#), [Rudoy et al. 2009](#)). This elicits reactivation of the associated memory representation, or rather intentionally biases this otherwise spontaneous process towards the memories

targeted by the procedure (e.g., [Bendor and Wilson 2012](#)). In humans, the manipulation has been found to be effective for both declarative ([Rasch et al., 2007](#); [Rudoy et al., 2009](#); [Fuentemilla et al., 2013](#)) and procedural ([Antony et al., 2012](#); [Schönauer et al., 2014](#); [Cousins et al., 2014, 2016](#)) memories, enhancing performance gains on the cued compared to the uncued task items.

Although TMR research has developed rapidly, becoming one of the most used sleep manipulation techniques, only a few studies have examined how the effects of TMR develop over time ([Hu et al., 2015](#); [Shanahan et al., 2018](#); [Groch et al., 2017](#); [Simon et al., 2018](#)). One of the most recent attempts was made by [Cairney et al. \(2018\)](#), where participants encoded pairwise associations, followed by three retrieval sessions: before and after a 90 min nap of cueing, and following a full night of sleep with no stimulation. While memory performance did not differ between cued and uncued pairs immediately after the nap, the memory-enhancing effect of TMR was evident the next morning. [Cairney et al. \(2018\)](#) argues that, during the TMR-induced windows of spindle-mediated memory processing, the synapses relevant for the task may be ‘tagged’ for plastic changes during subsequent sleep, hence uncovering TMR benefits the next day. Such a ‘tag’ could potentially also allow the cued memories to persist for longer than the uncued ones.

\* Corresponding author.

E-mail address: [rakowskam@cardiff.ac.uk](mailto:rakowskam@cardiff.ac.uk) (M. Rakowska).

<sup>1</sup> Present address: Experimental Psychopathology Lab, Institute of Psychology, Polish Academy of Sciences, Warsaw, Poland.

<sup>2</sup> Present address: Department of Biomedical Engineering, Universidad de los Andes, Bogotá, Colombia.

While long-term effects of TMR were first reported for implicit biases (Hu et al., 2015), neither object-location (Shanahan et al., 2018) nor emotional (Groch et al., 2017) memory seems to benefit a week after the manipulation. Procedural memory, on the other hand, has to our knowledge, never been investigated in this context.

Here, we set out to determine whether the memory-enhancing effects of TMR on motor memory consolidation (Antony et al., 2012; Schönauer et al., 2014; Cousins et al., 2014, 2016) persist over time, by using a bimanual serial reaction time task (SRTT) and investigating the difference between the cued and uncued sequence of button presses at different points in time. Participants learned two sequences of 12-item button presses, each associated with a different set of auditory tones. Tones associated with one of the sequences were replayed to the participants during subsequent sleep and the performance was re-tested 24 h, 10 days and ~6 weeks post-learning.

We delivered TMR in both stages 3 (N3) and 2 (N2) of NREM sleep due to procedural memory improvements reported following TMR delivery during N3 (Antony et al., 2012; Cousins et al., 2014, 2016) and N2 (Laventure et al., 2016, 2018). N3, also known as slow-wave sleep (SWS), has a well-established role in memory processing (Walker, 2009). It is the most common choice for declarative-memories TMR (Rasch et al., 2007; Rudoy et al., 2009; Diekelmann et al., 2012; Fuentemilla et al., 2013) as well as TMR in general (Hu et al., 2020). On the other hand, N2 has been consistently implied in motor sequence memory consolidation (Laventure et al., 2016; Nishida and Walker, 2007; Walker et al., 2002). Likewise, sleep spindles were shown to play an important role in procedural learning (Laventure et al., 2018; Barakat et al., 2011; Antony et al., 2012; Cousins et al., 2016; Nishida and Walker, 2007; Morin et al., 2008). Moreover, the interplay between the electrophysiological hallmarks of these two stages, i.e., the precise coupling between the amplitude of sleep spindles that characterise N2 and the phase of slow oscillations (SOs) that characterise N3, was shown to predict performance improvements for several memory tasks (Niknazar et al., 2015; Mikutta et al., 2019; Muehlroth et al., 2019; Hahn et al., 2020; Denis et al., 2020a; Schreiner et al., 2021). Hence, here we aimed to describe the electrophysiology for the two sleep stages with a particular focus on sleep spindles and their coupling with SOs, as well as to explore their relationship with TMR benefits for both hands and each hand separately, and at different points in time.

## 2. Materials and methods

### 2.1. Participants

Twenty-six healthy volunteers signed a written informed consent form to take part in the study, which was approved by the Ethics Committee of the School of Psychology at Cardiff University. All participants reported being right-handed, sleeping 6–9 h per night, having normal or corrected to normal vision and no hearing impairment. Subjects who had travelled across more than two time-zones or engaged in any regular night work one month prior to the experiment were not recruited for the study. Likewise, regular nappers and smokers did not take part. Further criteria for exclusion included recent stressful life event(s), prior history of drug/alcohol abuse, neurological, psychological, or sleep disorders. None of the participants reported taking any medication or substance directly or indirectly affecting sleep quality. Additionally, they were asked to abstain from napping, extreme physical exercise, caffeine, alcohol, and other psychologically active food from 24 h prior to each experimental session. We also excluded participants with more than three years of musical training in the past five years due to a probable link between musical abilities and procedural learning (Anaya et al., 2017; Romano Bergstrom et al., 2012). The experimental procedure was explained, and participants received instructions about the tasks, but no information was provided about the objectives of the study nor the variables of interest. All participants received monetary compensation for their time.

According to our inclusion criteria, participants must: (1) have no prior knowledge of the SRTT upon the start of the study; (2) undergo an uninterrupted TMR procedure; (3) show the SRTT error rate within 2 SD from the group mean during all sessions; (4) not classify as outliers using the outlier detection method from Cousins et al. (2014), applied to the both-hands dataset. Seven participants were excluded from analysis due to these criteria as follows: (1) sudden realisation that they had participated in a previous experiment that involved SRTT ( $n = 1$ ); (2) an interrupted TMR procedure caused by a high number of arousals throughout the night ( $n = 1$ ), or reference electrode failure before or during the stimulation ( $n = 2$ ); (3) a consistently high SRTT error rate throughout the study ( $> 2$  SD away from the group mean) ( $n = 1$ ); and (4) being classified as an outlier according to the SRTT outliers detection method from Cousins et al. (2014) which identified one participant ( $n = 1$ ) whose reaction time performance before sleep was  $> 2$  SD from group mean and one participant ( $n = 1$ ) for whom the disparity between the reaction time for the two sequences before sleep was  $> 2$  SD away from the group mean. One additional participant had to be removed from the dataset due to voluntary withdrawal ( $n = 1$ ).

Hence, the final dataset included 18 participants (10 females, age range: 18 - 22 years, mean  $\pm$ SD:  $19.7 \pm 1.2$ ; 8 males, age range: 18 - 24 years, mean  $\pm$ SD:  $21.1 \pm 1.7$ ). One of the participants ( $n = 1$ ) included in the dataset could not attend the last session and therefore the sample size for the analyses concerning the data collected during that session was 17. The final dataset also included two participants for whom part of the EEG data were missing due to EEG battery failure ( $n = 2$ ). However, the issue occurred after the TMR procedure had been completed. Thus, the two participants were included in all the analyses except for the sleep staging analysis, as it would be impossible to state the time these participants spent in each sleep stage with a few hours of the recording missing.

### 2.2. Study design

The study consisted of four sessions (Fig. 1A), all scheduled for the same time in the evening (~8pm). Session 1 (S1) lasted 3 h and was followed by a stimulation night in the sleep lab, during which participants slept with the electroencephalography (EEG) cap on. Upon arrival, participants first completed a series of questionnaires: short version of the Edinburgh Handedness Inventory (EHI) (Veale, 2014) to assess their handedness, Stanford Sleepiness Scale Questionnaire (SQ) (Hoddes et al., 1973) to determine their current level of alertness and Pittsburgh Sleep Quality Index (PSQI) (Buysse et al., 1989) to evaluate their sleep quality and quantity in the past month. Then, participants were asked to prepare themselves for bed before the wire up took place. With the EEG cap on, participants performed the SRTT and the imagery task. Noise-cancelling headphones (Sony MDR-ZX110NA, Sony Europe B.V., Surrey, UK) were used to deliver the tones during both tasks. Participants were ready for bed at ~11.30pm. During sleep (N2 and N3), the same tones were replayed to the participants through speakers (Harman/Kardon HK206, Harman/Kardon, Woodbury, NY, USA) to trigger reactivation of the associated SRTT memories. Participants were woken up at a time convenient for them (on average after  $8.46 \pm 0.45$  h in bed) and had the EEG cap removed. Before leaving the lab, they were asked whether they had heard any sounds during the night.

The remaining three follow up sessions lasted 40–60 min each and included behavioural testing only. Participants were asked to come back to the lab 23–25 h (session 2, S2), 6–11 days (session 3, S3) and 6–8 weeks (session 4, S4) after S1. During S2, S3 and S4 participants completed the SQ and the SRTT again. S4 also included an explicit memory task. Since the post-learning sleep was shown to enhance consolidation of memories expected to be retrieved (Wilhelm et al., 2011), participants were told to expect SRTT re-test upon completion of each experimental session.

All tasks/questionnaires were presented on a computer screen with resolution  $1920 \times 1080$  pixels, except for the explicit memory task, com-

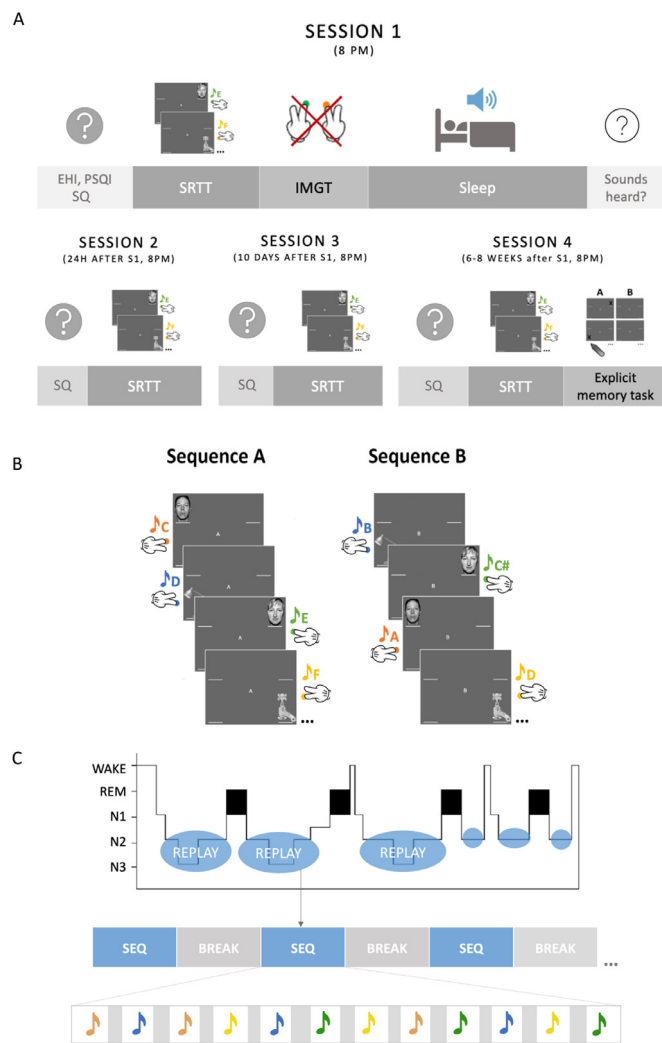


**Fig. 1.** Experimental methods. (A) Study design. The study consisted of four sessions, each requiring participants to complete one or more questionnaires and the SRTT. Session 1 also involved EEG recording during the main task, the imagery task (IMGT) and the overnight stay in the lab. During sleep, the TMR protocol was delivered. After waking up the next morning we asked participants whether they had heard any sounds during the night. In addition to the SQ and the SRTT, Session 4 also required participants to perform the explicit memory task. (B) A schematic representation of the two sequences of the SRTT. Auditory and visual cues appeared simultaneously. The tones had a fixed duration of 200 ms and were either high or low pitched depending on the counterbalancing condition. The visual cue remained on the screen until the correct key was pressed. The next trial appeared after a 300 ms inter-trial interval. (C) TMR protocol. Tones associated with one of the SRTT sequences were re-played to the participants in N3 and N2 (blue bubbles on the hypnogram). A single sequence (blue rectangles) was played, followed by a 20 s break (grey rectangles). Each sequence comprised 12 tones (here shown as coloured notes) with the inter-trial interval jittered between 2500 and 3500 ms (grey vertical bars). SRTT: Serial Reaction Time Task; IMGT: Imagery Task; EHI: Edinburgh Handedness Inventory; PSQI: Pittsburgh Sleep Quality Index; SQ: Stanford Sleepiness Scale Questionnaire (For interpretation of the references to color in this figure legend, the reader is referred to the web version of this article.).

pleted with pen and paper. Computer-based tasks were executed using MATLAB (The MathWorks Inc., Natick, MA, USA) and Cogent 2000 (developed by the Cogent 2000 team at the Functional Imaging Laboratory and the Institute for Cognitive Neuroscience, University College, London, UK; <http://www.vislab.ucl.ac.uk/cogent.php>). Questionnaires were executed using MATLAB and Psychophysics Toolbox Version 3 (Brainard, 1997).

## 2.3. Experimental tasks

### 2.3.1. Motor sequence learning-the serial reaction time task (SRTT)

The SRTT (Fig. 1B) was used to induce and measure motor sequence learning. It was adapted from Cousins et al. (2014) and consisted of two 12-item sequences of auditorily and visually cued key presses, learned by the participants in blocks. The sequences – A (1–2–1–4–2–3–4–1–3–2–4–3) and B (2–4–3–2–3–1–4–2–3–1–4–1) – were matched for learning difficulty, did not share strings of more than four items and contained items that were equally represented (three repetitions of each). Each sequence was paired with a set of 200 ms-long tones, either high (5th octave, A/B/C#/D) or low (4th octave, C/D/E/F) pitched, that were counterbalanced across sequences and participants. For each item/trial, the tone was played with simultaneous presentation of a visual cue in one of the four corners of the screen. Visual cues consisted of neutral faces and objects, appearing in the same location regardless of the sequences (1 – top left corner = male face, 2 – bottom left corner = lamp, 3 – top right corner = female face, 4 – bottom right corner = water tap). Participants were told that the nature of the stimuli (faces/objects) was not relevant for the study. Their task was to press the key on the keyboard that corresponded to the position of the picture as quickly and accurately as possible: 1 = left shift; 2 = left Ctrl; 3 = up arrow; 4 = down arrow. Participants were instructed to use both hands and always keep the same fingers on the appropriate response keys (1 = left middle finger, 2 = left index finger, 3 = right middle finger, 4 = right index finger). The visual cue disappeared from the screen only after the correct key was pressed, followed by a 300 ms interval before the next trial.

There were 24 blocks of each sequence (a total of 48 sequence blocks per session), where block type was indicated with ‘A’ or ‘B’ displayed in the centre of the screen. Each block contained three sequence repetitions (36 items) and was followed by a 15 s pause, with reaction time and error rate feedback. Blocks were interleaved pseudo-randomly with no more than two blocks of the same sequence in a row. Participants were aware that there were two sequences but were not asked to learn them explicitly. Block order and sequence replayed were counterbalanced across participants.

Following the 48 blocks of sequence A and B, participants performed 4 random blocks, indicated with ‘R’ appearing centrally on the screen. Those final blocks contained pseudo-randomised sequences, the same visual stimuli, and tones matching sequence A for half of them (Rand\_A) and sequence B for the other half (Rand\_B). Blocks Rand\_A and Rand\_B were interleaved, and the random sequences contained within them followed three constraints: (1) each cue was represented equally within a string of 12 items, (2) two consecutive trials could not contain the same cue, (3) random sequence did not share a string of more than four items with either sequence A or B.

### 2.3.2. Imagery task

Following the SRTT training, participants were instructed to do the same task again but without pressing any keys. Instead, they were told to imagine doing so, with their fingers resting immobile on the appropriate keys. The stimuli remained the same, except that the visual cues were presented for 880 ms and the inter-trial delay lasted 270 ms. The imagery task comprised 15 blocks of each sequence, with 5 s breaks in between but no performance feedback. The order of the sequence blocks was the same as during the SRTT but without the random blocks at the end.

### 2.3.3. Explicit memory task

To measure participants’ explicit memory of the SRTT, a free recall test was administered during the last experimental session. Participants were instructed to mark the sequence order on printed screenshots of the SRTT, arranged vertically in two columns and with the visual cues removed.

## 2.4. EEG data acquisition

EEG was recorded using 64 actiCap slim active electrodes (Brain Products GmbH, Gilching, Germany), with 62 electrodes embedded within an elastic cap (Easycap GmbH, Herrsching, Germany). This included the reference positioned at CPz and ground at AFz. The remaining electrodes were the left and right electrooculography (EOG) electrodes (placed below and above each eye, respectively), and left and right electromyography (EMG) electrodes (placed on the chin). Fig. S1 shows the EEG electrodes layout. Elefix EEG-electrode paste (Nihon Kohden, Tokyo, Japan) was used for stable electrode attachment and Super-Visc high viscosity electrolyte gel (Easycap GmbH) was inserted into each electrode to reduce impedance below 25 kOhm. To amplify the signal, we used either two BrainAmp MR plus EEG amplifiers or LiveAmp wireless amplifiers (all from Brain Products GmbH). Signals were recorded using BrainVision Recorder software (Brain Products GmbH).

## 2.5. TMR during NREM sleep

Tones associated with one of the learned sequences (A or B, counterbalanced across participants) were replayed to the participants during N2 and N3 (Fig. 1C), as assessed with standard AASM criteria (Berry et al., 2015). The TMR protocol was executed using MATLAB and Cogent 2000. Volume was adjusted for each participant to make sure that the sounds did not wake them up. One repetition of a sequence (i.e., 12 sounds) was followed by a 20 s break during which no sounds were played. The inter-trial interval within repetitions (i.e., between the sounds in a sequence) was jittered between 2500 and 3500 ms. Upon arousal or leaving the relevant sleep stage, replay was paused immediately and resumed only when stable N2/N3 was apparent. TMR was performed for as long as the minimum threshold of ~1000 trials in N3 was reached. On average, 1612.59 ( $\pm$ SD 162.20) sounds were delivered. The exact number of sounds played during each sleep stage was determined offline, with the results summarised in Table S1. Once the sleep scoring procedure was complete (see section 2.6.2.1 *Sleep Scoring* of this manuscript), the EEG data were cut into trials (defined as the time interval between cue onset and the end of the inter-trial interval) and if more than 50% of a trial fell within a given epoch, arousal or movement, that trial was deemed as being played during the respective period.

## 2.6. Data analysis

### 2.6.1. Behavioural data

**2.6.1.1. SRTT: reaction time.** Performance on the SRTT was measured using mean reaction time per block of each sequence (cued and uncued). Trials with reaction time > 1000 ms were excluded from the analysis; trials with incorrect button presses prior to the correct ones remained. Both hands (BH) dataset included all SRTT trials, left hand (LH) dataset included trials performed using left, non-dominant hand only, right hand (RH) dataset included trials performed using right, dominant hand only. Mean performance on 4 chosen blocks (see Fig. 2A, brown and grey vertical rectangles) was then subtracted from the mean performance on 2 random blocks to separate learning of the sequence from sensorimotor mapping, thus providing a measure of 'sequence-specific skill' (SSS). SSS was calculated for each sequence and session separately, using either the first 4 blocks (early SSS) or the last 4 blocks (late SSS). This is illustrated below, with higher outcome values indicating better performance:

- 1 Early sequence-specific skill (early SSS) = mean (random blocks) – mean (first 4 blocks)
- 2 Late sequence-specific skill (late SSS) = mean (random blocks) – mean (last 4 blocks)

Finally, we calculated the difference between the SSS of the cued and uncued sequence, thus obtaining a measure of 'cueing benefit', i.e.,

the effect of TMR on the SRTT performance, for each participant and at each timepoint.

**2.6.1.2. Questionnaires.** To identify outliers in the ordinal, PSQI and SQ datasets, a robust Modified Z-Score outlier detection method was used (Iglewicz and Hoaglin, 1993), calculated using the following formula:  $M_i = (0.6745 (x_i - \bar{x}))/MAD$ , where  $MAD = \text{median}\{|x_i - \bar{x}|\}$  and denotes Median Absolute Deviation. Any score above 3.5 would be considered an outlier and removed from the dataset. However, that was not the case for any of the questionnaires' measures. PSQI global scores were calculated according to the original scoring system described in Buysse et al. (1989). Handedness, i.e., laterality quotient based on the short version of the EHI, was scored as in Veale (2014).

**2.6.1.3. Explicit memory.** To assess the explicit memory of each sequence, individual items were scored as correct only if they were both (1) in the correct sequence position and (2) followed or preceded by at least one other correct item, hence minimising the effect of guessing as in Cousins et al. (2014). Chance level was determined by taking an average score of 10 randomly generated sequences per participant. The mean of those scores across all participants was considered the average number of items guessed by chance, which was then compared with the number of correct items for each sequence to determine if the explicit memory was formed.

### 2.6.2. EEG data analysis

All EEG data were analysed in MATLAB using FieldTrip Toolbox (Oostenveld et al., 2011).

**2.6.2.1. Sleep scoring.** EEG signal from eight scalp electrodes (F3, F4, C3, C4, P3, P4, O1, O2), two EOG and two EMG channels recorded throughout the night was pre-processed, re-referenced to the mastoids (TP9, TP10) and scored according to the standard AASM criteria (Berry et al., 2015). Scoring was performed by two trained and independent sleep scorers blind to the cue presentation periods using a custom-made interface (<https://github.com/mnavarretem/psgScore>).

**2.6.2.2. Spindles and slow waves detection.** The relationship between spindles and behavioural outcomes was determined by focusing the analysis on 8 electrodes located over motor regions: 4 left (FC3, C5, C3, C1, CP3) and 4 right (FC4, C6, C4, C2, CP4). However, for visualisation purpose, the rest of the electrodes in the International 10–20 EEG system were also pre-processed and analysed as outlined below, and included in the final figure (Fig. 5A). Briefly, the raw data were first down-sampled to 250 Hz (for them to be comparable between the two EEG data acquisition systems) and filtered using a Chebyshev Type II infinite impulse response (IIR) filter (passband:  $f = [0.3 - 35]$  Hz; stopband:  $f < 0.1$  Hz &  $f > 45$  Hz). Then, for each participant, the channels were visually inspected and, if deemed noisy for the majority of the night, interpolated based on their triangulation-based neighbours. The final pre-processing step involved re-referencing the data to the mastoids (TP9, TP10). Algorithms for spindles and SOs counting (Navarrete et al., 2020) were subsequently employed to detect slow oscillations (0.3 – 2 Hz) and sleep spindles (11 – 16 Hz) at each electrode and in each sleep stage separately (N2, N3) or combined (N2 and N3). Briefly, for spindles detection, the data were filtered in a sigma band using an IIR filter again (passband:  $f = [11 - 16]$  Hz; stopband:  $f < 9$  Hz &  $f > 18$  Hz). Then, we used a 300 ms time window to compute the root mean squared (RMS) of the signal. Any event that had surpassed the 86.64 percentile (1.5 SD, Gaussian distribution) of the RMS signal was regarded as a candidate spindle. To fit the final spindle detection criteria (based on Iber et al. 2007), an event was deemed a sleep spindle if it occurred in the target sleep stage, lasted between 0.5 and 2.0 s and had at least 5 oscillations during that period (Navarrete et al., 2020). For SOs detection, the EEG data were filtered in the 0.3 – 2 Hz band using the IIR filter (passband:  $f = [0.3 - 2]$  Hz; stopband:  $f < 0.1$  Hz &  $f > 4$  Hz). Waves with negative deflection

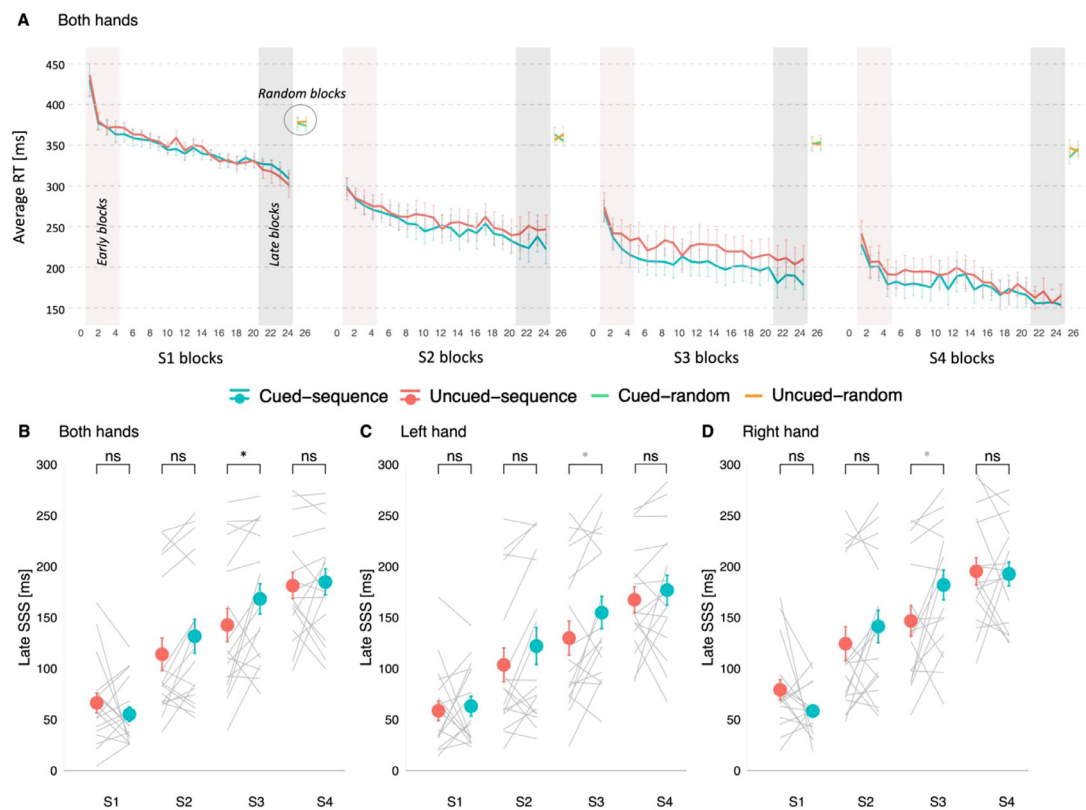


**Fig. 2.** (A) Mean reaction time [ms] for the BH trials of the cued (blue) and uncued (red) sequence blocks as well as random blocks (green and orange) during all experimental sessions (S1–S4). Error bars represent SEM. Vertical rectangles highlight the first (brown) and last (grey) four blocks of each sequence used to calculate the early and late SSS, respectively. (B–D) TMR affects late SSS performance on Session 3 (S3), regardless of the hand analysed. Mean late SSS for BH (B), LH (C) and RH (D) dataset plotted against time (S1–S4). Red dots represent mean  $\pm$ SEM for the uncued sequence. Blue dots represent mean  $\pm$ SEM for the cued sequence. Grey lines represent performance of each subject. Although not marked with p-values, the participants showed significant improvements with time on both the cued and the uncued sequence. ns: non-significant; \* $p < 0.05$ , uncorrected; when adjusted for multiple comparisons using Holm's correction the effect of TMR on S3 remained significant only for (B) (black \*) but not for (C) or (D) (grey \*).  $n = 18$  for S1–S3,  $n = 17$  for S4. S1–4: Session 1–4; SSS: Sequence Specific Skill. BH: both hands; LH: left hand; RH: right hand (For interpretation of the references to color in this figure legend, the reader is referred to the web version of this article.).

between  $-35$  and  $-300$  mV and with zero crossing between 0.13 and 1.66 s were considered SOs. The identified spindles and SOs were then separated into those that fell within the cue and no-cue periods. The cue period was defined as the time interval between 0 and 3.5 s after a tone onset (the longest inter-trial interval allowed), thus essentially encompassing the period from the onset of the first tone in a sequence until 3.5 s after the onset of the last one. The no-cue period was defined as the time interval between the sequences - from 3.5 to 20.0 s after the onset of the last tone in the sequence.

Spindle density was calculated by dividing the total number of spindles at each electrode by the length (in minutes) of the target period (cue period during target sleep stage, no-cue period during target sleep stage). Spindle density, together with the number of spindle and SO events during the cue and no-cue period of each of the target sleep stages, are presented in Table S2. Spindle laterality was obtained by subtracting spindle density over the right motor channels from the spindle density over the left motor channels.

**2.6.2.3. Phase amplitude coupling.** Trial-based phase-amplitude coupling was calculated for each channel using mean resultant length (MRL), as described in Canolty et al. (2006). Similarly to the spindle analysis, the statistical analyses concerning the phase-amplitude coupling measures were performed on the 8 motor electrodes (FC3, C5, C3, C1, CP3, FC4, C6, C4, C2, CP4), with the rest of the electrodes in the International 10–20 EEG system analysed only for visualisation purpose (Fig. 6A). In short, the phase and amplitude evolving timeseries was filtered using a zero-shift IIR filter in delta (passband:  $f = [0.3 -$

$2]$  Hz; stopband:  $f < 0.1$  Hz &  $f > 4$  Hz) and sigma (passband:  $f = [11 - 16]$  Hz; stopband:  $f < 9$  Hz &  $f > 18$  Hz) bands, respectively. Hilbert transform was then applied to obtain the instantaneous frequency of the delta- and sigma- filtered signal. Phase-amplitude coupling was computed for concurrent SO and spindles detected using the methods described above (2.6.2.2 *Spindles and slow waves detection*). The number of SO-spindle events detected during the cue and no-cue period of each of the target sleep stages is presented in Table S2. MRL was then estimated to assess how well spindles align to the same phase of the SO. MRL equal to 0 reflects no coupling (i.e., random distribution of spindles in a slow wave cycle), whereas MRL equal to 1 reflects maximal coupling (i.e., all spindles occurring at precisely the same time of every slow wave cycle). For clarity, the measure is later referred to as the coupling strength. The coupling strength was compared to a set of surrogate data (200 permutations), created by shifting the amplitude evolving time series by a randomised time lag from the phase evolving time series. This allowed us to assess the significance of coupling and define a normalised, or z-scored, coupling strength (CS) as below:

$CS_n = (CS_{raw} - \mu) / \sigma$ , where  $\mu$  and  $\sigma$  denote the mean and standard deviation of surrogate's coupling strength, respectively. The normalised coupling strength is used throughout this report. To obtain the coupling phase, i.e., the phase of the SO which the spindles best align to, the phase of the SO cycle was cut into 100 equally spaced bins between  $-\pi$  to  $\pi$  radians. The average amplitude of each phase bin was then calculated for the amplitude evolving time series, and the circular mean was computed from the circular distribution to obtain the final value for the

coupling phase. The coupling phase plots (Fig. S3) were created using the CircStat toolbox in MATLAB (Berens, 2009).

Finally, both the mean of the coupling strength and the circular mean of the coupling phase (in degrees) were calculated for all motor channel, left motor channels and right motor channels to obtain the coupling strength and phase over both hemispheres, left and right hemisphere, used in the further analyses.

### 2.6.3. Statistical analysis

Statistical analysis was performed in MATLAB, the R environment (R Core Team, 2012) or SPSS Statistics 25 (IBM Corp., Armonk, NY, USA). Each dataset (LH, RH, BH), stimulation period (cue vs no-cue) and sleep stage (N2, N3, N2 and N3 combined) was analysed separately. Normality assumption was checked using Shapiro-Wilk test and all tests conducted were two-tailed, with the significance threshold set at 0.05. Results are presented as mean  $\pm$  standard error of the mean (SEM), unless otherwise stated.

To compare two related samples, we used paired-samples t-tests (Gaussian distribution), Wilcoxon signed-rank test (non-Gaussian distribution) or Watson-Williams test (circular data). Correlations between EEG data and behavioural measures were tested with either Pearson's correlation (Gaussian distribution) or Spearman's Rho (non-Gaussian distribution) using the `cor.test` function in the R environment, or using the `circ_corrl` function in the CircStat toolbox (Berens, 2009) if correlations between circular and linear variables were evaluated. If a given datapoint within a linear variable was more than 1.5 interquartile ranges (IQRs) below the first quartile or above the third quartile, and if it was deemed an outlier through visual inspection, that datapoint was removed from the dataset before the correlational analysis. Multiple correlations were corrected using false discovery rate (FDR) correction ( $q < 0.05$ ) (Benjamini and Hochberg, 1995), thus controlling for the expected proportion of falsely rejected hypotheses. The corrections were based on a total of 3 correlations, given the 3 sessions of interest (S2, S3, S4).

To test the relationship between SSS, TMR and Session we used linear mixed effects analysis to account for the non-independence of multiple responses collected from the participants over time, as well as to avoid listwise deletion due to missing data in S4. The analysis was performed on S2-S4 using lme4 package in R (Bates et al., 2012). For both late and early SSS, TMR and Session were entered into the model as fixed effects (without interaction) and random intercept was specified for each subject. The final models for BH, LH and RH dataset were as follows:

```
> model = lmer(SSS ~ Session + TMR + (1|Participant), data = dataset)
```

To assess the effect of hand, LH and RH datasets were combined and the model fitted to the data also included hand as one of the fixed effects:

```
> model = lmer(SSS ~ Session + TMR + Hand + (1|Participant),
  data = dataset)
```

Finally, to explore how the TMR effect evolves over time (i.e., between S2 and S4) we fitted the following model to each dataset, with cueing benefit as the dependant variable. This analysis was performed on the 'late' cueing benefit only (i.e., calculated using the late SSS data), as no TMR effect was found for the early SSS.

```
> model = lmer(CueingBenefit ~ Session + (1|Participant), data = dataset)
```

The model fitted to the LH and RH datasets combined, again, also included hand as one of the fixed effects:

```
> model = lmer(CueingBenefit ~ Session + Hand + (1|Participant),
  data = dataset)
```

Likelihood ratio tests of the full model against the model without the effect being tested were used to obtain the p-values. When a significant difference was found, post-hoc pairwise comparisons of least-squares

means with Holm adjustment were conducted using the emmeans package in R (Lenth et al., 2019). The emmeans package was also used to calculate the effect sizes.

## 2.7. Data and code availability

All the data used in the study as well as the software and scripts used to present the experimental tasks to the participants and to perform the analysis have been made publicly available via the Open Science Framework and can be accessed at: [https://osf.io/kxspw/?view\\_only=25ca3eca34004df496302c9dc1cc7580](https://osf.io/kxspw/?view_only=25ca3eca34004df496302c9dc1cc7580).

## 3. Results

### 3.1. Questionnaires

The EHI confirmed that all participants were right-handed, as the laterality quotient score (ranging between  $-100$  and  $+100$ , where the negative values indicate left-handers and positive right-handers) was  $+100\%$  for all but one subject who scored  $+75\%$ . PSQI global scores (on a 21-points scale) ranged between 2 and 6 points across participants, with a mean of  $4.33 (\pm 0.32)$ , indicating, on average, a 'good quality' of sleep (Buysse et al., 1989). The median answer on the SQ (with 1 and 9 indicating the highest and lowest level of alertness, respectively) was 2 for all sessions ( $\pm$ IQR for S1: 1, S2: 2, S3: 1, S4: 1), indicating similar levels of alertness throughout the study.

Participants did report hearing experimental sounds during the night. On a 3-points scale, the median answer was 3 (IQR: 2), with 28% of the participants not hearing any sounds (answer 1), 11% of the participants being unsure (answer 2), and 61% of the participants hearing them clearly (answer 3). However, when asked about the number of sounds they had heard, the median answer was 3 (IQR: 3.5) sounds and only 17% of the subjects reported hearing more than 6 sounds.

### 3.2. SRTT

#### 3.2.1. Reaction time and sequence specific skill

Before sleep, no difference was found between the average reaction time of the cued and uncued sequence for either BH ( $t_{17} = -0.35$ ,  $p = 0.729$ ), LH ( $t_{17} = -1.02$ ,  $p = 0.321$ ) or RH ( $t_{17} = 0.38$ ,  $p = 0.710$ ) dataset (paired-samples t-tests for all comparisons). Similar results were obtained when comparing random sequences before sleep for all datasets (BH:  $Z = -0.63$ ,  $p = 0.528$ ; LH:  $Z = -0.72$ ,  $p = 0.472$ ; RH:  $Z = -0.68$ ,  $p = 0.500$ ; Wilcoxon signed-rank test). Thus, any post-sleep difference between the sequences can be regarded as the effect of TMR. Furthermore, average reaction times before sleep were significantly shorter for the last 4 sequence blocks than the random blocks, confirming that the participants learned both sequences during S1 (BH cued:  $Z = -3.72$ ; BH uncued:  $Z = -3.72$ ; LH cued:  $Z = -3.59$ ; LH uncued:  $Z = -3.72$ ; RH cued and uncued:  $Z = -3.68$ ;  $p < 0.001$  for all comparisons, Wilcoxon signed-rank test). Summary statistic for each sequence and dataset during S1 are presented in Table 1. Mean reaction time ( $\pm$  SEM) for the BH trials of each block during the full course of the study is shown in Fig. 2A.

Post-sleep SRTT re-test sessions took place 23.89 h (SD: 0.47) (S2), 9.89 days (SD: 1.02) (S3), and 43.94 days (SD: 4.43) (S4) after S1. To examine the effect of TMR on SSS (either early or late) over time (S2-S4) we performed a linear mixed effects analysis on each dataset (BH, LH, RH) separately. Results of all the likelihood ratio tests of the full model (with TMR and session as fixed effects and participant as a random effect) against the model without the fixed effect of interest are presented in Table S3A-C. No effect of TMR was revealed for the early SSS (Table S3Ai-Ci) and therefore we will focus only on the late SSS (Table S3Aii-Cii) for the rest of this report. Likewise, even though we found a main effect of hand on the SRTT performance ( $p < 0.001$ ; Table S3D, better performance for the dominant hand), the analysis revealed

**Table 1**  
SRTT summary statistics.

Dataset	Cued sequence	Uncued sequence	Cued random	Uncued random	Cued sequence (last 4 blocks)	Uncued sequence (last 4 blocks)
BH	346.64 ± 6.80	347.93 ± 6.86	375.27 ± 7.19	378.55 ± 4.97	320.13 ± 7.13	312.32 ± 11.41
LH	358.02 ± 8.22	362.97 ± 7.34	384.50 ± 9.00	387.33 ± 6.82	328.85 ± 7.84	328.78 ± 11.23
RH	335.28 ± 6.08	332.90 ± 7.40	366.04 ± 6.79	369.83 ± 5.00	311.35 ± 7.74	295.86 ± 12.33

Mean reaction time ( $\pm$  SEM) (in ms) for the BH, LH and RH trials of the cued and uncued sequence blocks (24 per sequence) as well as random blocks (2 with tones matching the cued and 2 with tones matching the uncued sequence) during Session 1. Average reaction time ( $\pm$  SEM) for the last 4 blocks of each sequence are shown as well. BH: both hands; LH: left hand; RH: right hand.  $n = 18$ .

similar results for all datasets (BH: Table S3–5A, LH: Table S3–5B, RH: Tables S3–5C), with no interaction between either hand and session or hand and TMR ( $p > 0.05$ ; Table S3D). Thus, we will report findings for the BH dataset only.

The analysis revealed that the inclusion of session as a fixed effect significantly improves model fit ( $X^2(2) = 47.66$ ,  $p < 0.001$ ), pointing to the main effect of session on the late SSS (Table S3Aii). Post-hoc tests showed a difference ( $p_{\text{adj}} < 0.001$ ) between both S2 and S3, and S3 and S4, suggesting that the participants were getting significantly faster with each session (Table S4Aii).

When the full model was tested against the model without TMR, the likelihood ratio test revealed that the inclusion of TMR as a fixed effect significantly improves model fit for late SSS ( $X^2(1) = 6.87$ ,  $p = 0.009$ ) across all sessions (S2–S4) (Table S3Aii). The interaction between TMR and session was, however, not significant ( $X^2(2) = 2.39$ ,  $p = 0.303$ ) (Table S3Aii). The linear mixed effects analysis therefore suggested a main effect of TMR on late SSS. Given our previous findings on this task (Cousins et al., 2014, 2016; Koopman et al., 2020), we expected higher performance for the cued than uncued sequence on S2 but sought to determine if that is also true for the remaining sessions. Hence, we carried out post-hoc pairwise comparisons to reveal the session(s) during which TMR significantly affected the SRTT performance. To our surprise, we found a significant effect of TMR on S3 ( $p_{\text{adj}} = 0.045$ ) but no difference between the cued and uncued sequence performance on S2 ( $p_{\text{adj}} = 0.179$ ) or S4 ( $p_{\text{adj}} = 0.743$ ) (Table S5A, Fig. 2B–D). The absence of a TMR effect at S2 could be explained by the fact that our second session occurred in the evening (24 h post-stimulation), while both Cousins et al. (2014, 2016) and Koopman et al. (2020) who report significant findings on the same task retested their participants in the morning (12 h post-stimulation). Nevertheless, the TMR effect seems to (re-)emerge following subsequent nights of sleep (i.e., at day 10 post-stimulation) but does not last until 6 weeks later.

### 3.2.2. Cueing benefit across time

To explore how the TMR effect evolves over time, we compared the difference between the late SSS of the cued and uncued sequence (i.e., the cueing benefit) across sessions (S2–S4) using the linear mixed effects analysis. Inclusion of session as the fixed effect revealed a trend for improved model fit for the BH dataset ( $\chi^2(2) = 5.89$ ,  $p = 0.053$ ; Table S6A), a significantly better model fit for the RH dataset ( $\chi^2(2) = 6.77$ ,  $p = 0.034$ ; Table S6C) but no model improvement for the LH dataset ( $\chi^2(2) = 2.31$ ,  $p = 0.314$ ; Table S6B). We carried out post-hoc pairwise comparisons to reveal the sessions between which the cueing benefit differed. While the cueing benefit was similar between S2 and S3 (BH:  $p_{\text{adj}} = 0.347$ , RH:  $p_{\text{adj}} = 0.334$ ), we found a difference between S3 and S4 for both datasets (BH:  $p_{\text{adj}} = 0.034$ , RH:  $p_{\text{adj}} = 0.026$ ) (Table S7, Fig. 3A,C). These results suggest a benefit of TMR 10 days post-manipulation which then decreases with time. Interestingly, there was neither a main effect of hand nor an interaction between hand and session ( $p > 0.05$ ; Table S6D).

### 3.3. Explicit memory task

Given that TMR was shown to promote the emergence of explicit knowledge the next morning (Cousins et al., 2014), we also set out

**Table 2**  
Sleep parameters.

	Percentage of total recording duration [%]	Mean duration $\pm$ SEM [min]
Total recording duration	100%	525.13 $\pm$ 10.56
Total sleep time	89.74%	469.66 $\pm$ 9.27
Wake	10.26%	55.47 $\pm$ 9.50
N1	5.76%	30.34 $\pm$ 5.35
N2	41.65%	219.56 $\pm$ 12.28
N3	21.89%	113.13 $\pm$ 7.38
REM	18.78%	97.72 $\pm$ 6.22
Movement	1.54%	8.22 $\pm$ 1.56

Total recording duration, total sleep time, time spent in each sleep stage and time scored as movement presented as average (minutes  $\pm$  SEM) and as percentage of the total recording duration. Total sleep time was calculated by subtracting the time spent in wake from the total recording duration. N1–N3: stage 1 - stage 3 of NREM sleep.  $n = 16$ .

to test whether this is true after a longer period. However, we found no difference between the free recall of the cued and uncued sequence ( $Z = -1.29$ ,  $p = 0.196$ , Wilcoxon signed-rank test), suggesting no TMR effect on the explicit knowledge of the sequence ~6 weeks post-encoding (Fig. S2). Nevertheless, performance on both sequences differed from chance (cued:  $Z = -3.39$ ,  $p < 0.001$ ; uncued:  $Z = -3.43$ ,  $p < 0.001$ ; Wilcoxon signed-rank test), indicating that the participants learned both sequences explicitly over the course of the experiment.

### 3.4. Correlations with sleep stages

All sleep parameters obtained through sleep scoring are summarised in Table 2. To test whether there was any relationship between sleep characteristics and the TMR effect we correlated the time spent in N2 and N3 (the two target stages for our stimulation) with the cueing benefit at S2, S3 and S4, and for each dataset (BH, LH, RH) separately. All correlational results are presented in Table S8. The percentage of time spent in N2 showed a positive correlation with the cueing benefit at S4 for BH ( $R = 0.65$ ,  $p_{\text{adj}} = 0.045$ , Fig. 4A) and LH ( $R = 0.68$ ,  $p_{\text{adj}} = 0.027$ , Fig. 4B) and with the cueing benefit at S2 for RH ( $R = 0.66$ ,  $p_{\text{adj}} = 0.018$ , Fig. 4C). In other words, the time spent in N2 (but not N3) predicts TMR benefit for the dominant hand earlier (24 h post-TMR) than for the non-dominant hand or both hands combined (6 weeks post-TMR).

### 3.5. Sleep spindles

Sleep spindles, i.e., short bursts of activity in sigma (11–16 Hz) frequency band, are the EEG signatures characteristic of N2 (Purcell et al., 2017). Thus unsurprisingly, the average spindle density over the task related regions in N2 was significantly higher than in N3, but only during the cue (N2:  $4.39 \pm 0.46$  vs N3:  $3.75 \pm 0.39$ ;  $z = -2.765$ ,  $p = 0.006$ ) and not the no-cue period (N2:  $3.62 \pm 0.43$  vs N3:  $3.47 \pm 0.47$ ;  $z = -0.370$ ,  $p = 0.711$ ; Wilcoxon signed-rank test). Furthermore, for N2, the average spindle density during the cue period ( $4.39 \pm 0.46$ ) was significantly higher than during the no-cue period ( $3.62 \pm 0.43$ ) ( $z = -2.81$ ,  $p = 0.005$ ; Wilcoxon signed-rank test, Fig. 5). This, however, was not the case for N3 (cue:  $3.75 \pm 0.40$  vs no-cue:  $3.47 \pm 0.47$ ;  $z = -1.42$ ,

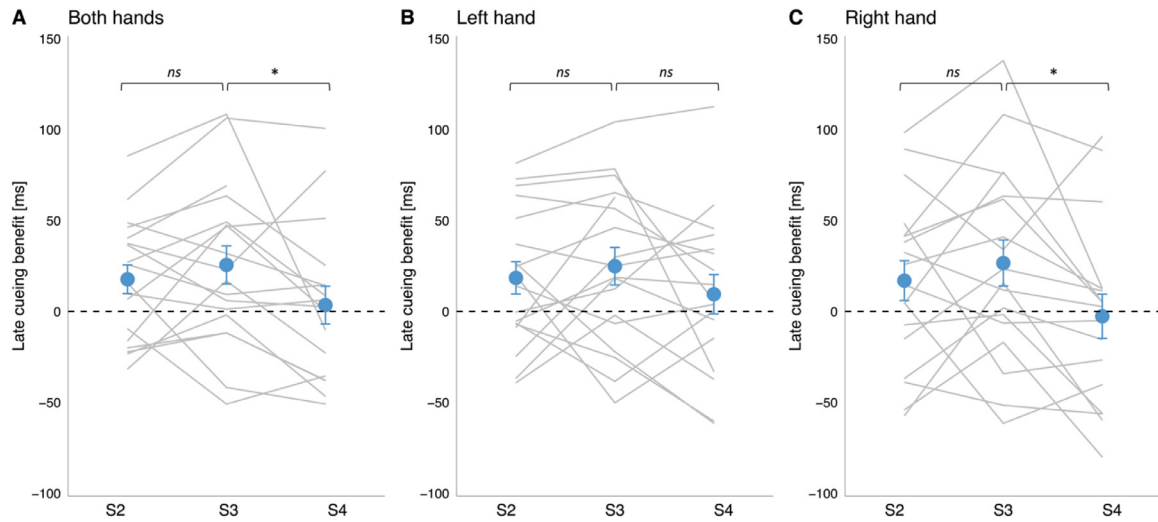


**Fig. 3.** Cueing benefit over time. Mean late SSS on the uncued sequence subtracted from the cued sequence for both hands (A), left hand (B) and right hand (C), plotted against time (S2-S4). The effect of time was trending towards significance for (A) and reached significance for (C), with the post-hoc comparisons revealing a difference between S3 and S4 in both cases. Blue dots represent mean  $\pm$ SEM. Grey lines represent TMR effect for each subject.  $n = 18$  for S2-S3;  $n = 17$  for S4. S2-4: Session 2-4; ns: non-significant,  $*p < 0.05$  (For interpretation of the references to color in this figure legend, the reader is referred to the web version of this article.).

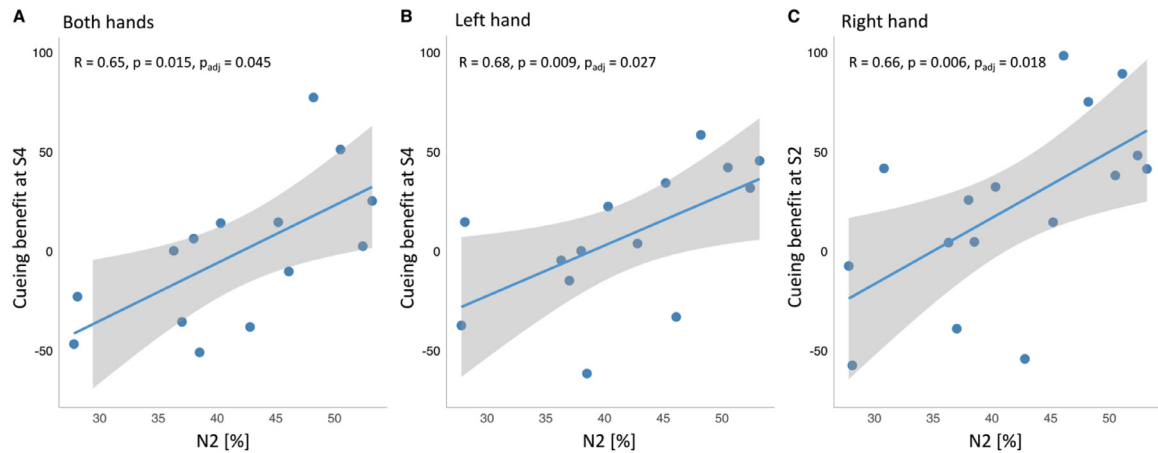


**Fig. 4.** Positive correlation between the percentage of time spent in N2 and the cueing benefit (late SSS for the uncued sequence subtracted from the cued sequence) at S4 for both hands (A) and left hand (B), and at S2 for right hand (C). Grey bands around the regression line represent confidence intervals. Both the uncorrected p-values and the p-values adjusted for multiple comparisons are shown. S4: Session 4, S2: Session 2, N2: stage 2 of NREM sleep; SSS: Sequence Specific Skill.  $n = 14$  for (A,B) and  $n = 16$  for (C).

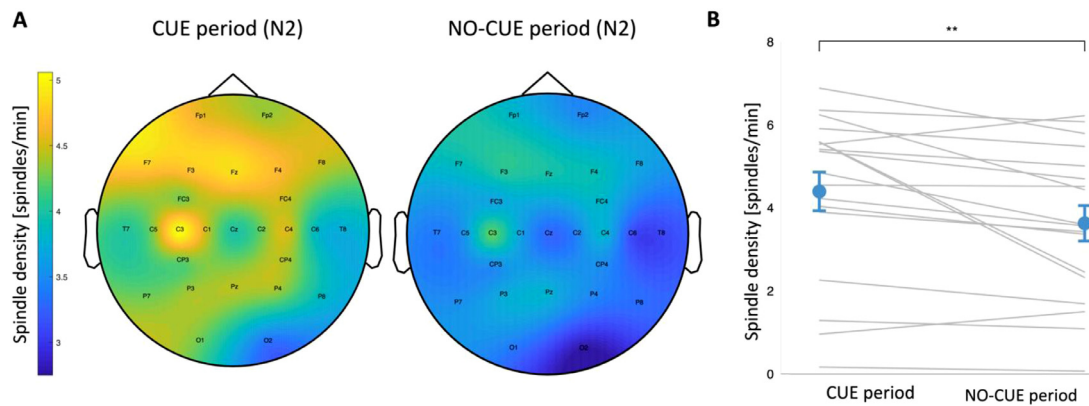


**Fig. 5.** (A) Topographic distribution of spindle density (spindles per min) in N2 and N3 of the cue (left) and no-cue (right) period. (B) Spindle density averaged over motor channels (4 left: FC3, C5, C3, C1, CP3 and 4 right: FC4, C6, C4, C2, CP4) during N2 was significantly higher during the cue period than during the no-cue period.  $**p = 0.005$ . N2-N3: stage 2 - stage 3 of NREM sleep.  $n = 18$ .



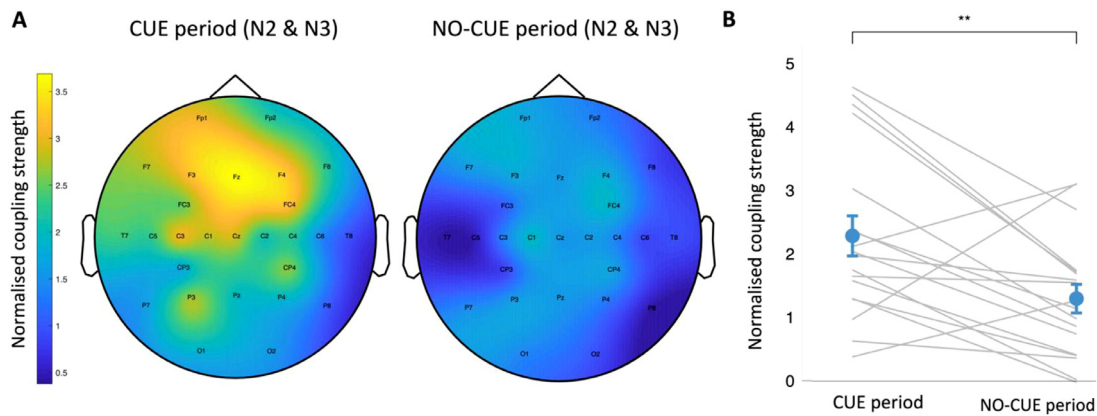


**Fig. 6.** (A) Topographic distribution of the normalised (z-scored) strength of the SOs-spindle coupling during N2 and N3 of the cue (left) and no-cue (right) period. (B) Coupling strength over motor channels (4 left: FC3, C5, C3, C1, CP3 and 4 right: FC4, C6, C4, C2, CP4) for N2 and N3 was significantly higher during the cue period than during the no-cue period.  $**p = 0.009$ . N2–N3: stage 2 – stage 3 of NREM sleep.  $n = 18$ .

$p = 0.157$ ; Wilcoxon signed-rank test). When the two stages (N2 and N3) were combined, the spindle density averaged over the left motor areas was significantly higher than over the right motor areas, both during the cue (left:  $3.84 \pm 0.42$  vs right:  $3.44 \pm 0.38$ ;  $t(17) = 3.84$ ,  $p = 0.001$ ) and no-cue period (left:  $3.36 \pm 0.44$  vs right:  $2.95 \pm 0.40$ ;  $t(17) = 3.77$ ,  $p = 0.002$ ; paired-samples  $t$ -test). This result could relate to the fact that participants performed better on the task using their right hand, contralateral to the site of the local spindle density increase, as shown before (Nishida and Walker, 2007; Cousins et al., 2014). Overall, these results suggest that cueing may elicit sleep spindles in N2, but not in N3. The immediate surge in spindle density upon stimulation in N2 could then be followed by a subsequent reduction after the cue period. This would explain the similar levels of spindle density in N2 and N3 observed during the no-cue period.

The literature reports spindle-related changes over brain areas involved in learning (Cox et al., 2014) which often predict behavioural improvements (Bergmann et al., 2012; Lutz et al., 2021; Fogel et al., 2017; Barakat et al., 2013). Thus, to test whether sleep spindles relate to the cued sequence advantage in our study, we correlated cueing benefit for S2–S4 with spindle density, averaged over motor electrodes. Since we found no main effect of hand on the cueing benefit, only the BH dataset was analysed. Given the differential role of sleep spindles during different stages of NREM sleep (Cox et al., 2012; Dehnavi et al., 2019), spindles in N2 and N3 were analysed both together and separately. Nevertheless, there was no correlation surviving FDR correction ( $p_{\text{adj}} > 0.05$ ; Table S9).

Previous studies using similar procedural learning tasks report a relationship between spindle laterality and behavioural outcomes (Cousins et al., 2014; Nishida and Walker, 2007). Even though the task used in this study was bilateral, rather than unilateral as in Nishida and Walker (2007) and Cousins et al. (2014), we found higher spindle density over the left vs right motor areas. Thus, we were interested to test whether lateralised spindle density (calculated by subtracting spindle density over the right motor channels from spindle density over the left motor channels) correlate with the cueing benefit of either hand (especially the right hand, contralateral to the left hemisphere). N2 and N3 were analysed both separately and combined, as before, with all the results reported in Table S10. We found that during the cue period (N2 and N3 combined), spindle laterality trended strongly towards a positive correlation with the cueing benefit in the BH dataset at S4 ( $R = 0.56$ ,  $p = 0.017$ ,  $p_{\text{adj}} = 0.051$ , Fig. S3). No other correlation between spindle laterality and cueing benefit was revealed ( $p_{\text{adj}} > 0.05$ ). This could suggest that lateralised spindles that occur over the task-related regions and during the cue period may be able to predict long-term cueing benefit for both hands, however this should be treated with caution given that it did not survive FDR correction.

### 3.6. Phase amplitude coupling

According to the active systems consolidation theory, memory reactivation (and thus consolidation) involves a coordinated interplay, or coupling, of hippocampal sharp-wave ripples, neocortical slow waves and thalamocortical sleep spindles (Rasch and Born, 2013). At the scalp EEG level, coupling between the phase of SOs and amplitude of sleep spindles (phase-amplitude coupling) was linked to performance improvements on several memory tasks (Niknazar et al., 2015; Mikutta et al., 2019; Muehlroth et al., 2019; Hahn et al., 2020; Denis et al., 2020a; Schreiner et al., 2021), but not (yet) with the SRTT. Thus, we sought to investigate phase-amplitude coupling during N2 and N3, and its relationship with our behavioural outcomes from the SRTT.

Coupling strength was higher in N3 than in N2 both for the cue (N2:  $1.09 \pm 0.21$  vs N3:  $2.07 \pm 0.34$ ;  $z = -2.59$ ,  $p = 0.010$ ) and the no-cue period (N2:  $0.38 \pm 0.14$  vs N3:  $1.39 \pm 0.18$ ;  $z = -3.64$ ,  $p < 0.001$ ) (Wilcoxon signed-rank test). For N2 and N3 combined, we found no difference in coupling strength between the two hemispheres (cue period:  $z = -1.02$ ,  $p = 0.306$ ; no-cue period:  $z = -0.72$ ,  $p = 0.472$ ; Wilcoxon signed-rank test). However, coupling strength was significantly higher during the cue period than during the no-cue period (cue:  $2.29 \pm 0.32$  vs no-cue:  $1.30 \pm 0.23$ ;  $z = -2.61$ ,  $p = 0.009$ ; Wilcoxon signed-rank test; Fig. 6). This suggests that cueing may increase the strength of SO-spindle coupling during both N2 and N3.

Regarding the coupling phase, i.e., the phase of the SO which the spindles best align to, with the peak of the SO set at  $0^\circ$ , no significant differences were revealed. Specifically, we found no difference between the coupling phase in N2 and N3 (cue:  $F_{1,35} = 0.843$ ,  $p = 0.365$ ; no-cue:  $F_{1,35} = 2.05$ ,  $p = 0.162$ ), no difference between the coupling phase over the left and right motor regions (cue period:  $F_{1,35} = 0.08$ ,  $p = 0.774$ ; no-cue period:  $F_{1,35} = 1.16$ ,  $p = 0.288$ ), and no difference between the cue and no-cue period (N2:  $F_{1,35} = 0.05$ ,  $p = 0.820$ ; N3:  $F_{1,35} = 0.29$ ,  $p = 0.591$ ; N2 and N3:  $F_{1,35} = 1.11$ ,  $p = 0.300$ , Fig. S4) (Watson-Williams test for all comparisons).

We then correlated coupling strength with cueing benefit for S2–S4, both during the cue and no-cue period. Given that coupling strength did not differ between left and right hemispheres, it was averaged over all motor channels (both hemispheres), and correlated with the BH dataset (Table S11). Unexpectedly, the analysis did not reveal any correlation between cueing benefit at S3 and coupling strength during the cue period ( $p_{\text{adj}} > 0.05$ ). Instead, we found a negative correlation between cueing benefit at S2 and coupling strength during the no-cue period, only in N2 ( $R = -0.59$ ,  $p_{\text{adj}} = 0.036$ , Fig. S5). Although the correlation could be of interest to future studies, it is hard to justify given both the existing literature and our findings so far. Furthermore, we found no correlation between cueing benefit and coupling phase ( $p_{\text{adj}} > 0.05$ ,

Table S12), leaving the relationship between SO-spindle coupling and behavioural performance open to debate.

#### 4. Discussion

In this study we primarily aimed to investigate how the memory-enhancing effects of TMR on procedural skill learning develop over time, with a particular focus on the SRTT. Participants continued to improve on the SRTT over the total course of the study (6 weeks), with significantly higher performance from one session to the next, regardless of the hand used. Overall, participants were also significantly better on the task with their dominant (right) than the non-dominant (left) hand. When all post-stimulation sessions were combined, a main effect of TMR was apparent. This was true regardless of whether the hands were analysed together or separately, but only for late SSS, with no difference for early SSS. Closer examination revealed that late SSS was comparable between sequences 24 h post-manipulation but was greater for the cued than the uncued sequence 10 days later. Six weeks after stimulation the TMR effect had disappeared from all datasets. Furthermore, we found a main effect of session on the cueing benefit: while the TMR advantage was comparable between the first two time points post-stimulation, it decreased from 10 days to 6 weeks post-TMR. Thus, our results show a benefit of TMR 10 days post-manipulation which then decreases with time.

We sought to describe the electrophysiology of N2 and N3 (the two target sleep stages for our stimulation) as well as determine whether sleep spindles and their coupling with SOs could predict the behavioural benefits of TMR. These analyses revealed that (1) the time spent in N2, but not N3, predicts cueing benefit; (2) there is a significant increase in both the average spindle density and coupling strength immediately after cue presentation, as compared to a later time period.

##### 4.1. TMR effect evolves over time

We showed a main effect of TMR on the late SRTT performance across all post-sleep sessions. However, the difference between the cued and uncued sequence was the strongest at 10 days post-encoding, thus driving the main effect. The absence of a clear TMR effect the day after stimulation was unexpected, given that it was apparent on the day after stimulation in prior studies (Cousins et al., 2014, 2016; Koopman et al., 2020). This difference could have occurred because our second session was scheduled in the evening rather than in the morning, immediately after a full night of sleep (as in previous studies), thus also preventing direct comparison with literature. Alternatively, the reason for the delayed effects could be the jittering of the TMR cues during sleep. Jittering was introduced instead of a fixed inter-trial duration to allow better characterisation of temporal features of memory reactivation. However, this also disrupted the temporal dynamics of the cueing, since the brain could no longer predict when the next cue was due to arrive. Prior work has confirmed that cueing specifically acts to consolidate the sequence (Cousins et al., 2014, 2016), and such temporally unpredictable cueing may have made it harder to consolidate the transitions which make up the sequence. Indeed, internalising the regularity of events optimises stimulus processing and allows faster learning (Nobre et al., 2007). Therefore, randomising the timing of cues, as opposed to previous studies that used constant intervals between cues (Cousins et al., 2014, 2016; Koopman et al., 2020), could have delayed the behavioural effects of stimulation.

The significant TMR effect at 10 days post-manipulation suggests that TMR starts a process which unfolds over several days after stimulation. This is consistent with Cairney et al. (2018) who argue that synapses relevant for the task are ‘tagged’ for plastic changes during sleep following cue presentation, allowing the cueing benefits to persist. Alternatively, synapses relevant for both the cued and uncued sequence may be ‘tagged’ at encoding, priming them for further plastic changes that occur during sleep over the course of several subsequent nights

(Seibt and Frank, 2019; Pereira and Lewis, 2020). This process could be facilitated by cue presentation for one of the sequences, allowing its memory trace to persist for longer. In other words, cue presentation could have preferentially strengthened the cued memory trace which thereby allowed it to be remembered for longer and gave rise to the observed effect. Thus, what we here termed as the ‘cueing benefit’ could be simply regarded as the difference between the strengths of two traces and their differential decay time.

The disappearance of the TMR effect at our last experimental session suggests that the TMR-related plasticity does not last until, or beyond, 6 weeks. Furthermore, the absence of any TMR benefit to explicit knowledge at 6 weeks is in keeping with the idea that all the TMR benefits fade by this time. This is not surprising given that neither object-location (Shanahan et al., 2018) nor emotional (Groch et al., 2017) memory seems to benefit from the manipulation even a week later. Alternatively, the loss of TMR effect at S4 could have been caused by a ceiling effect which prevented further improvement on the task, and thus allowed the slower consolidating uncued sequence to catch up with the faster consolidating cued sequence. Indeed, by the end of the study the average reaction time on the sequence blocks was below 200 ms, which is lower than reported by other SRTT studies with less training sessions (Koopman et al., 2020; Cousins et al., 2014; Romano et al., 2010). On the other hand, Verstynen et al. (2012), who used a far more intensive study design than we did, showed that lower reaction times are possible on the same task. The study reports continuous behavioural improvements across 10 days of SRTT training (5 weekdays for 2 weeks) with reaction time reaching less than 100 ms by the tenth session (Verstynen et al., 2012). Nevertheless, the reaction times reported in the literature are not exactly comparable due to several differences in the task design (e.g., different number of trials, blocks or hands used) and, to our knowledge, the ceiling values have not yet been estimated. Assuming that the ceiling has not been reached and given the difference in cueing benefit between 10 days and 6 weeks post-stimulation, our data suggest that the TMR benefit is present at 10 days post-stimulation, and then decreases across the days that follow until it disappears altogether. Unfortunately, regardless of the reason for the loss of cueing effect at 6 weeks, the maximum duration of the TMR impact remains unknown. Future research should thus attempt to understand this process more fully, and to determine the extent of time for which TMR can impact memories, both the explicit and implicit ones. It will also be interesting to see how these parameters vary across declarative and procedural tasks.

##### 4.2. TMR benefits both hands

Even though the overall performance on the task was significantly better for the dominant than the non-dominant hand, data from both hands yielded similar results with respect to TMR. There was also no interaction between hand and TMR across time, or significant effect of hand on the cueing benefit. These findings were counter to our expectation, since weaker memory representations with a lot of room for improvement have been shown to be more responsive to TMR than the strongly remembered ones (Cairney et al., 2016; Drosopoulos et al., 2007; Schapiro et al., 2018; Tambini et al., 2017). Hence, we expected the non-dominant (i.e., ‘weaker’) hand to benefit more from the stimulation than the dominant one. Given our findings from this and a previous study (Koopman et al., 2020), one possibility could be that TMR is indeed more beneficial for the non-dominant hand, but only at first. The effect of TMR on the dominant hand could then catch up within 24 h post-learning, thus making it impossible for us to observe any difference between the hands at our first re-test session which occurred 24 h after the initial training. Another, more probable explanation is that the handedness effect is so subtle that the results are strongly dependant on individual variations. With two experimental sessions, 14 participants in the RH and 13 in the LH dataset, Koopman et al. (2020) found a significant TMR x time interaction for left but not right hand, although a qualitative trend was apparent for the latter. Here, with more power (four

experimental sessions, 18 participants in the RH and LH dataset), we report a significant main effect of TMR for both datasets. Nevertheless, further investigation into the effect of handedness is warranted, with a particular focus on the first 24 h post-manipulation. Studies analogous to this one but using left-handed individuals could determine whether our findings can be generalised from the right-handed sample to the whole population.

Despite the fact that both hands benefitted from TMR, cueing benefit for the dominant hand was predicted by N2 earlier (24 h post-TMR) than cueing benefit for the non-dominant hand (6 weeks post-TMR). This could suggest distinct consolidation processes for the two hands. Interestingly, time spent in N3 did not predict cueing benefit. This difference highlights the importance of N2 in procedural memory consolidation, in line with prior work (Smith and MacNeill, 1994; Smith et al., 2004; Korman et al., 2007; Fogel and Smith 2006; Fogel et al., 2007). It also suggests that N2 may be a better choice than N3 for this TMR.

#### 4.3. Relationship between EEG features and TMR benefits

We found a significant increase in the average spindle density (N2) and coupling strength (both N2 and N3) during the cue period (0–3.5 s after cue onset) as compared to the no-cue period (3.5–20 s after the onset of the last cue in the sequence). This suggests that auditory stimulation can perhaps boost sleep oscillations and thereby induce an immediate processing of memory traces. Our results are consistent with other TMR studies, namely Antony et al. (2018) which reports spindle density increase early (0–2 s) relative to later (2–4 s) after TMR cues, and Cairney et al. (2018) which likewise observes a surge in spindle activity (modulated by the SO up-state) 1.7 to 2.3 s after cue onset. Both Antony et al. (2018) and Cairney et al. (2018) linked the cue-induced spindle activity increase to memory reactivation during sleep, as well as behavioural performance at retest.

## 5. Conclusions

We provide the first report on the long-term impact of TMR on procedural skill learning. While previous studies showed cueing effects lasting for up to a week (Hu et al., 2015; Simon et al., 2018), our findings are the first to suggest that TMR over one night of sleep can affect procedural memories as far as 10 days post-stimulation, with effects lost by six weeks post-stimulation. Furthermore, we show that time in N2 but not N3 predicts TMR benefit. Finally, both spindle density and SO-spindle coupling strength increase upon cue onset, thus drawing attention to the rapid memory processing which may be happening at that time. Future investigation of the mechanisms underlying long-term impact of TMR, including the plastic changes induced by such manipulation, will help us to build an understanding of the complex processes linked to memory reactivation in sleep.

#### Data and code availability statement

All the data used in the study as well as the software and scripts used to present the experimental tasks to the participants and to perform the analysis have been made publicly available via the Open Science Framework and can be accessed at: [https://osf.io/kxspw/?view\\_only=25ca3eca34004df496302c9dc1cc7580](https://osf.io/kxspw/?view_only=25ca3eca34004df496302c9dc1cc7580).

#### Declaration of Competing Interest

The authors have no conflict of interest to disclose.

#### Credit authorship contribution statement

**Martyna Rakowska:** Conceptualization, Project administration, Investigation, Formal analysis, Data curation, Visualization, Writing –

original draft. **Mahmoud E.A. Abdellahi:** Conceptualization, Investigation, Writing – review & editing. **Paulina Bagrowska:** Investigation, Formal analysis, Writing – review & editing. **Miguel Navarrete:** Software, Methodology, Writing – review & editing. **Penelope A. Lewis:** Conceptualization, Supervision, Funding acquisition, Writing – review & editing.

#### Acknowledgements

The authors would like to thank Anne Koopman, Holly Kings, Sofia Pereira and Lorena Santamaria-Covarrubias for helpful comments and discussion on this manuscript, as well as Niall McGinley and Ibad Kashif for their help with participants' recruitment and sleep scoring. We also thank all the participants for their time and commitment to the study.

#### Funding

This work was funded by the ERC grant SolutionSleep, 681607, to PL.

#### Supplementary materials

Supplementary material associated with this article can be found, in the online version, at doi:10.1016/j.neuroimage.2021.118573.

#### References

- Anaya, E.M., Pisoni, D.B., Kronenberger, W.G., 2017. Visual-spatial sequence learning and memory in trained musicians. *Psychol. Music* 45 (1), 5–21.
- Antony, J.W., Gobel, E.W., O'Hare, J.K., Reber, P.J., Paller, K.A., 2012. Cued memory reactivation during sleep influences skill learning. *Nat. Neurosci.* 15 (8), 1114–1116.
- Antony, J.W., Piloto, L., Wang, M., Pacheco, P., Norman, K.A., Paller, K.A., 2018. Sleep spindle refractoriness segregates periods of memory reactivation. *Curr. Biol.* 28 (11), 1736–1743.
- Barakat, M., Carrier, J., Debas, K., Lungu, O., Fogel, S., Vandewalle, G., ... Doyon, J., 2013. Sleep spindles predict neural and behavioral changes in motor sequence consolidation. *Hum. Brain Mapp.* 34 (11), 2918–2928.
- Barakat, M., Doyon, J., Debas, K., Vandewalle, G., Morin, A., Poirier, G., ... Carrier, J., 2011. Fast and slow spindle involvement in the consolidation of a new motor sequence. *Behav. Brain Res.* 217 (1), 117–121.
- Bates, D., Maechler, M., Bolker, B. (2012). lme4: Linear mixed-effects models using Eigen and Eigen. R package version 0.999999-0. Available online at: <https://cran.r-project.org/web/packages/lme4/index.html>.
- Bendor, D., Wilson, M.A., 2012. Biasing the content of hippocampal replay during sleep. *Nat. Neurosci.* 15 (10), 1439.
- Benjamini, Y., Hochberg, Y., 1995. Controlling the false discovery rate: a practical and powerful approach to multiple testing. *Journal of the Royal statistical society: series B (Methodological)* 57 (1), 289–300.
- Berens, P., 2009a. CircStat: a MATLAB toolbox for circular statistics. *J. Stat. Softw.* 31 (1), 1–21.
- Berens, P., 2009b. CircStat: a MATLAB toolbox for circular statistics. *J. Stat. Softw.* 31 (10), 1–21.
- Bergmann, T.O., Mölle, M., Diedrichs, J., Born, J., Siebner, H.R., 2012. Sleep spindle-related reactivation of category-specific cortical regions after learning face-scene associations. *Neuroimage* 59 (3), 2733–2742.
- Berry, R.B., Gamaldo, C.E., Harding, S.M., Brooks, R., Lloyd, R.M., Vaughn, B.V., Marcus, C.L., 2015. AASM scoring manual version 2.2 updates: new chapters for scoring infant sleep staging and home sleep apnea testing. *J. Clin. Sleep Med.* 11 (11), 1253–1254.
- Born, J., Rasch, B., Gais, S., 2006. Sleep to remember. *Neuroscientist* 12 (5), 410–424.
- Brainard, D.H., 1997. The psychophysics toolbox. *Spat. Vis.* 10 (4), 433–436.
- Buyse, D.J., Reynolds, C.F., Monk, T.H., Berman, S.R., Kupfer, D.J., 1989. The Pittsburgh Sleep Quality Index: a new instrument for psychiatric practice and research. *Psychiatry Res.* 28 (2), 193–213.
- Cairney, S.A., El Marj, N., Staresina, B.P., 2018. Memory consolidation is linked to spindle-mediated information processing during sleep. *Curr. Biol.* 28 (6), 948–954.
- Cairney, S.A., Lindsay, S., Sobczak, J.M., Paller, K.A., Gaskell, M.G., 2016. The benefits of targeted memory reactivation for consolidation in sleep are contingent on memory accuracy and direct cue-memory associations. *Sleep* 39 (5), 1139–1150.
- Canolty, R.T., Edwards, E., Dalal, S.S., Soltani, M., Nagarajan, S.S., Kirsch, H.E., ... Knight, R.T., 2006. High gamma power is phase-locked to theta oscillations in human neocortex. *Science* 313 (5793), 1626–1628.
- Cousins, J.N., El-Derey, W., Parkes, L.M., Hennies, N., Lewis, P.A., 2014. Cued memory reactivation during slow-wave sleep promotes explicit knowledge of a motor sequence. *J. Neurosci.* 34 (48), 15870–15876.
- Cousins, J.N., El-Derey, W., Parkes, L.M., Hennies, N., Lewis, P.A., 2016. Cued reactivation of motor learning during sleep leads to overnight changes in functional brain activity and connectivity. *PLoS Biol.* 14 (5).

- Cox, R., Hofman, W.F., Talamini, L.M., 2012. Involvement of spindles in memory consolidation is slow wave sleep-specific. *Learn. Mem.* 19 (7), 264–267.
- Cox, R., Hofman, W.F., de Boer, M., Talamini, L.M., 2014. Local sleep spindle modulations in relation to specific memory cues. *Neuroimage* 99, 103–110.
- Dehnavi, F., Moghimi, S., Sadrabadi Haghighi, S., Safaie, M., Ghorbani, M., 2019. Opposite effect of motivated forgetting on sleep spindles during stage 2 and slow wave sleep. *Sleep* 42 (7), zsz085.
- Denis, D., Mylonas, D., Poskanzer, C., Bursal, V., Payne, J.D., Stickgold, R., 2020a. Sleep spindles facilitate selective memory consolidation. *BioRxiv*.
- Diekelmann, S., Born, J., 2010. The memory function of sleep. *Nat. Rev. Neurosci.* 11, 114–126.
- Diekelmann, S., Biggel, S., Rasch, B., Born, J., 2012. Offline consolidation of memory varies with time in slow wave sleep and can be accelerated by cuing memory reactivations. *Neurobiol. Learn. Mem.* 98 (2), 103–111.
- Drosopoulos, S., Schulze, C., Fischer, S., Born, J., 2007. Sleep's function in the spontaneous recovery and consolidation of memories. *J. Exp. Psychol. Gen.* 136 (2), 169.
- Dudai, Y., 2012. The restless engram: consolidations never end. *Annu. Rev. Neurosci.* 35, 227–247.
- Fogel, S.M., Smith, C.T., 2006. Learning-dependent changes in sleep spindles and Stage 2 sleep. *J. Sleep Res.* 15 (3), 250–255.
- Fogel, S.M., Smith, C.T., Cote, K.A., 2007. Dissociable learning-dependent changes in REM and non-REM sleep in declarative and procedural memory systems. *Behav. Brain Res.* 180 (1), 48–61.
- Fogel, S., Albouy, G., King, B.R., Lungu, O., Vien, C., Bore, A., ... Doyon, J., 2017. Re-activation or transformation? Motor memory consolidation associated with cerebral activation time-locked to sleep spindles. *PLoS ONE* 12 (4), e0174755.
- Fuentemilla, L., Miró, J., Ripollés, P., Vilà-Balló, A., Juncadella, M., Castañer, S., ... Rodríguez-Fornells, A., 2013. Hippocampus-dependent strengthening of targeted memories via reactivation during sleep in humans. *Curr. Biol.* 23 (18), 1769–1775.
- Gais, S., Born, J., 2004. Declarative memory consolidation: mechanisms acting during human sleep. *Learn. Mem.* 11 (6), 679–685.
- Groch, S., Preiss, A., McMakin, D.L., Rasch, B., Walitza, S., Huber, R., Wilhelm, I., 2017. Targeted reactivation during sleep differentially affects negative memories in socially anxious and healthy children and adolescents. *J. Neurosci.* 37 (9), 2425–2434.
- Hahn, M.A., Heib, D., Schabus, M., Hoedlmoser, K., Helfrich, R.F., 2020. Slow oscillation-spindle coupling predicts enhanced memory formation from childhood to adolescence. *Elife* 9, e53730.
- Hoddes, E., Zarcone, V., Smythe, H., Phillips, R., Dement, W.C., 1973. Quantification of sleepiness: a new approach. *Psychophysiology* 10 (4), 431–436.
- Hu, X., Antony, J.W., Creery, J.D., Vargas, I.M., Bodenhausen, G.V., Paller, K.A., 2015. Unlearning implicit social biases during sleep. *Science* 348 (6238), 1013–1015.
- Hu, X., Cheng, L.Y., Chiu, M.H., Paller, K.A., 2020. Promoting memory consolidation during sleep: a meta-analysis of targeted memory reactivation. *Psychol. Bull.* 146 (3), 218.
- Iber, C., Ancoli-Israel, S., Chesson, A.L., Quan, S.F., 2007. *The AASM Manual For the Scoring of Sleep and Associated events: rules, Terminology and Technical Specifications* (Vol. 1). American academy of sleep medicine, Westchester, IL.
- Iglewicz, B., Hoaglin, D., 1993. How to Detect and Handle outliers, 16. *The ASQC Basic References in Quality control: Statistical techniques* (Doctoral dissertation, Ph. D., Editor).
- Koopman, A.C., Abdellahi, M.E., Belal, S., Rakowska, M., Metcalf, A., Sledziowska, M., Hunter, T., Lewis, P., 2020. Targeted memory reactivation of a serial reaction time task in SWS, but not REM, preferentially benefits the non-dominant hand. *bioRxiv*.
- Korman, M., Doyon, J., Doljansky, J., Carrier, J., Dagan, Y., Karni, A., 2007. Daytime sleep condenses the time course of motor memory consolidation. *Nat. Neurosci.* 10 (9), 1206–1213.
- Laventure, S., Fogel, S., Lungu, O., Albouy, G., Sévigny-Dupont, P., Vien, C., ... Doyon, J., 2016. NREM2 and sleep spindles are instrumental to the consolidation of motor sequence memories. *PLoS Biol.*
- Laventure, S., Pinsard, B., Lungu, O., Carrier, J., Fogel, S., Benali, H., ... Doyon, J., 2018. Beyond spindles: interactions between sleep spindles and boundary frequencies during cued reactivation of motor memory representations. *Sleep* 41 (9), zsy142.
- Lenth, R., Singmann, H., Love, J., Buerkner, P., Herve, M. (2019). *Emmeans: estimated Marginal Means, aka Least-Squares Means* (Version 1.3. 4). Available online at: <https://cran.r-project.org/web/packages/emmeans/index.html>.
- Loganathan, R., 2014. The Role of Sleep in Motor Learning. *PostDoc J.* 2 (4), 18–29.
- Lutz, N.D., Admard, M., Genzoni, E., Born, J., Rauss, K., 2021. Occipital sleep spindles predict sequence learning in a visuo-motor task. *Sleep*.
- Mikutta, C., Feige, B., Maier, J.G., Hertenstein, E., Holz, J., Riemann, D., Nissen, C., 2019. Phase-amplitude coupling of sleep slow oscillatory and spindle activity correlates with overnight memory consolidation. *J. Sleep Res.* 28 (6), e12835.
- Morin, A., Doyon, J., Dostie, V., Barakat, M., Tahar, A.H., Korman, M., ... Carrier, J., 2008. Motor sequence learning increases sleep spindles and fast frequencies in post-training sleep. *Sleep* 31 (8), 1149–1156.
- Muehlroth, B.E., Sander, M.C., Fandakova, Y., Grandy, T.H., Rasch, B., Shing, Y.L., Werkle-Bergner, M., 2019. Precise slow oscillation–spindle coupling promotes memory consolidation in younger and older adults. *Sci. Rep.* 9 (1), 1–15.
- Navarrete, M., Schneider, J., Ngo, H.V.V., Valderrama, M., Casson, A.J., Lewis, P.A., 2020. Examining the optimal timing for closed-loop auditory stimulation of slow-wave sleep in young and older adults. *Sleep* 43 (6), zsz315.
- Niknazar, M., Krishnan, G.P., Bazhenov, M., Mednick, S.C., 2015. Coupling of thalamocortical sleep oscillations are important for memory consolidation in humans. *PLoS ONE* 10 (12), e0144720.
- Nishida, M., Walker, M.P., 2007. Daytime naps, motor memory consolidation and regionally specific sleep spindles. *PLoS ONE* 2 (4), e341.
- Nobre, A. C., Correa, A., Coull, J. T., 2007. The hazards of time.. *Current opinion in neurobiology* 17 (4), 465–470.
- Oostenveld, R., et al., 2011. FieldTrip: open source software for advanced analysis of MEG, EEG, and invasive electrophysiological data. *Comput. Intell. Neurosci.* 2011.
- Peigneux, P., Laureys, S., Fuchs, S., Collette, F., Perrin, F., Reggers, J., ... Luxen, A., 2004. Are spatial memories strengthened in the human hippocampus during slow wave sleep? *Neuron* 44 (3), 535–545.
- Pereira, S.I.R., Lewis, P.A., 2020. The differing roles of NREM and REM sleep in the slow enhancement of skills and schemas. *Curr. Opin. Physiol.* 15, 82–88.
- Purcell, S.M., Manoach, D.S., Demanuele, C., Cade, B.E., Mariani, S., Cox, R., ... Redline, S., 2017. Characterizing sleep spindles in 11,630 individuals from the National Sleep Research Resource. *Nat. Commun.* 8 (1), 1–16.
- R Core Team, 2012. R: a language and environment for statistical computing. R Foundation for Statistical Computing. R Foundation for Statistical Computing, Vienna, Au, Vienna, Austria.
- Rasch, B., Born, J., 2013. About sleep's role in memory. *Physiol. Rev.* 93, 681–766.
- Rasch, B., Büchel, C., Gais, S., Born, J., 2007. Odor cues during slow-wave sleep prompt declarative memory consolidation. *Science* 315 (5817), 1426–1429.
- Romano Bergstrom, C. J., C. J., Jr, Howard, J., H., Howard, D.V., 2012. Enhanced implicit sequence learning in college-age video game players and musicians. *Appl. Cogn. Psychol.* 26 (1), 91–96.
- Romano, J.C., Howard, J.H., Howard, D.V., 2010. One-year retention of general and sequence-specific skills in a probabilistic, serial reaction time task. *Memory* 18 (4), 427–441.
- Rudoy, J.D., Voss, J.L., Westerberg, C.E., Paller, K.A., 2009. Strengthening individual memories by reactivating them during sleep. *Science* 326 (5956), 1079–1079.
- Schapiro, A.C., McDevitt, E.A., Rogers, T.T., Mednick, S.C., Norman, K.A., 2018. Human hippocampal replay during rest prioritizes weakly learned information and predicts memory performance. *Nat. Commun.* 9 (1), 1–11.
- Schönauer, M., Geisler, T., Gais, S., 2014. Strengthening procedural memories by reactivation in sleep. *J. Cogn. Neurosci.* 26 (1), 143–153.
- Schreiner, T., Petzka, M., Staudigl, T., Staresina, B.P., 2021. Endogenous memory reactivation during sleep in humans is clocked by slow oscillation-spindle complexes. *Nature communications* 12 (1), 1–10.
- Seibt, J., Frank, M.G., 2019. Primed to sleep: the dynamics of synaptic plasticity across brain states. *Front. Syst. Neurosci.* 13, 2.
- Shanahan, L.K., Gjorgieva, E., Paller, K.A., Kahnt, T., Gottfried, J.A., 2018. Odor-evoked category reactivation in human ventromedial prefrontal cortex during sleep promotes memory consolidation. *Elife* 7, e39681.
- Simon, K.C., Gómez, R.L., Nadel, L., 2018. Losing memories during sleep after targeted memory reactivation. *Neurobiol. Learn. Mem.* 151, 10–17.
- Smith, C.T., Aubrey, J.B., Peters, K.R., 2004. Different roles for REM and stage 2 sleep in motor learning: a proposed model. *Psychol. Belg.* 44, 81–104.
- Smith, C., MacNeill, C., 1994. Impaired motor memory for a pursuit rotor task following Stage 2 sleep loss in college students. *J. Sleep Res.* 3 (4), 206–213.
- Tambini, A., Berners-Lee, A., Davachi, L., 2017. Brief targeted memory reactivation during the awake state enhances memory stability and benefits the weakest memories. *Sci. Rep.* 7 (1), 1–17.
- Veale, J.F., 2014. Edinburgh handedness inventory—short form: a revised version based on confirmatory factor analysis. *Later. AsymmetrieBody Brain Cognit.* 19 (2), 164–177.
- Verstynen, T., Phillips, J., Braun, E., Workman, B., Schunn, C., Schneider, W., 2012. Dynamic sensorimotor planning during long-term sequence learning: the role of variability, response chunking and planning errors. *PLoS ONE* 7 (10).
- Walker, M.P., 2009. The role of slow wave sleep in memory processing. *J. Clin. Sleep Med.* JCSM Off. Publ. Am. Acad. Sleep Med. 5 (2 Suppl), S20.
- Walker, M.P., Brakefield, T., Morgan, A., Hobson, J.A., Stickgold, R., 2002. Practice with sleep makes perfect: sleep-dependent motor skill learning. *Neuron* 35 (1), 205–211.
- Wilhelm, I., Diekelmann, S., Molzow, I., Ayoub, A., Mölle, M., Born, J., 2011. Sleep selectively enhances memory expected to be of future relevance. *J. Neurosci.* 31 (5), 1563–1569.
- Wilson, M.A., McNaughton, B.L., 1994. Reactivation of hippocampal ensemble memories during sleep. *Science* 265 (5172), 676–679.